Zinc Binding to Amyloid-β: Isothermal Titration Calorimetry and Zn Competition Experiments with Zn Sensors†

Christine Talmard, Anaïs Bouzan, and Peter Faller*

Laboratoire de Chimie de Coordination, CNRS UPR 8241, University Toulouse III, 205 route de Narbonne, 31077 Toulouse Cedex 4, France

Received July 10, 2007; Revised Manuscript Received September 11, 2007

ABSTRACT: Aggregation of the peptide amyloid-β (Aβ) to amyloid plaques is a key event in Alzheimer's disease. According to the amyloid cascade hypothesis, Aβ aggregates are toxic to neurons via the production of reactive oxygen species and are hence directly involved in the cause of the disease. Zinc ions play an important role, because they are able to bind to Aβ and influence the aggregation properties. In the present work isothermal titration calorimetry and Zn sensors (zincon, Newport Green, and zinquin) were used to investigate the interaction of Zn with the full-length Aβ1−40 and Aβ1−42, as well as the truncated Aβ1−16 and Aβ1−28. The results suggest that Zn binding to Aβ induces a release of ∼0.9 proton by the peptide. This correspond to the expected value upon Zn binding to the three histidines and indicates that further ligands are not deprotonated upon Zn binding. Such behavior is expected for carboxylates, but not the N-terminus. Moreover, the apparent dissociation constant ($K_{d,app}$) of Zn binding to all forms of Aβ is in the low micromolar range (1−20 μM) and rather independent of the aggregation state including soluble Aβ, Aβ fibrils, or Zn-induced Aβ aggregates. Finally, Zn in the soluble or aggregated Zn−Aβ form is well accessible for Zn chelators. The potential repercussions on metal chelation therapy are discussed.

The aggregation of the peptide amyloid-β (Aβ) into fibrils is considered to be a key event in Alzheimer's disease (*1*−*4*). In vivo, the most prevalent forms of Aβ consist of 40 (Aβ40)[1] and 42 (Aβ42) amino acids. Aβ is cleaved from the membrane protein amyloid precursor protein (APP). The longer form Aβ42 is more prone to aggregation and more toxic to neurons than Aβ40. This is in agreement with the widely accepted amyloid cascade hypothesis, which proposes that an increased Aβ accumulation and aggregation lead to the formation of fibrils in amyloid plaques and to neuronal disfunction and later on dementia (*2*). However, it is thought that soluble, oligomeric forms of Aβ are the most toxic species, rather than more aggregated fibrils or protofibrils (*2*). In this context, factors influencing this aggregation are of high interest (*5*). Studies in vitro, in cell cultures, and in AD model mice indicate an important role for metals (Zn, Cu, and Fe) in this respect (*1*, *4*, *6*, *7*).

In the case of Zn, a large body of evidence has been accumulated supporting an important role of this metal ion in the metabolism of Aβ linked to Alzheimer's disease. Zn has been found in the amyloid plaques at high concentrations (∼mM), and treatment with chelators partially solubilized the plaques (*8*). APP possesses a high-affinity Zn-binding site, which is located outside the Aβ region (*9*, *10*). Transgenic mice, which express human APP, develop amyloid plaque pathology and then can serve as models for AD. In such mice the lack of the Zn transporter ZnT3 (transports Zn into synaptic vesicles) reduced the plaque load. Hence, it was concluded that endogenous Zn contributed to the amyloid deposition in transgenic mice (*11*). Chelators, such as clioquinol, DP109, and cyclo-phen-type, known to bind Zn (and Cu) reduced successfully the amyloid plaque burden in transgenic mice (*7*, *12*−*15*).

In vitro studies revealed that Zn binds to Aβ and promotes its aggregation (*5*, *16*, *17*). Zn binds to Aβ in a monomeric and stoichiometric Zn−Aβ complex, which is transiently stable prior to aggregation (*18*). Moreover, Zn binding also influences the morphology of the Aβ aggregates. Generally their structures were described to be more amorphous, i.e., containing no or less fibrils. Zn-induced aggregates are less reactive with the marker thioflavin T than aggregates formed in the absence of Zn (*19*−*23*).

The first Zn-binding site of Aβ is located in the N-terminal part. Researchers in several studies on soluble Aβ40 or truncated forms containing the Zn-binding site (i.e., Aβ16 and Aβ28) tried to identify the ligands of Zn in Aβ (*19*, *24*−*34*). Although there is some contradiction, the involvement of histidines 6, 13, and 14 has been suggested in most studies. Less agreement is found concerning further ligands. Mostly suggested was the aspartate at position 1, by either the N-terminus or carboxylate side chain (*28*, *29*, *34*). In the case of an acetylated N-terminus, an NMR structure of Zn−Aβ1−16 was solved and showed that Zn is bound to the three His residues and Glu11 (*31*). Less is known for

† This work was supported by a grant from the French ministry, ACI-INTERFACE PCB (DRAB). C.T. was supported by a grant from ESF.

* To whom correspondence should be addressed. Phone: +33 5 61 33 31 62. Fax: +33 5 61 55 30 03. E-mail: peter.faller@lcc-toulouse.fr.

[1] Abbreviations: Aβ16, amyloid-β1−16; Aβ28, amyloid-β1−28; Aβ40, amyloid-β1−40; Aβ42, amyloid-β1−42; HEPES, {2-(4-(2-hydroxyethyl)-1-piperazinyl)ethanesulfonic acid; ITC, isothermal titration calorimetry; $K_{d,app}$, apparent dissociation constant; Tris, tris-(hydroxymethyl)aminomethane.

10.1021/bi701355j CCC: $37.00
Published on Web 11/06/2007

the Zn-binding site in Zn-induced aggregates of Aβ. Raman spectroscopy studies indicated that it is provided by three His residues similar to soluble Aβ (*25*). In contrast, EXAFS measurements detected differences between soluble and aggregated Aβ, among others the number of His residues involved (*32*). It has also been suggested that the peptide aggregates through intermolecular His(N(τ))−Zn^{II}−His(N(τ)) bridges (*25*). Concerning Zn binding to Aβ fibrils formed in the absence Zn, to our best knowledge no information is available.

A key parameter in the interaction of Zn with Aβ is the affinity for the metal. The knowledge of the dissociation constant allows the comparison with other biological and nonbiological Zn ligands. This can give insights into the possible sources of Zn ions able to be chelated by Aβ, as well as which ligands (proteins or others) would be able to withdraw Zn from Aβ. This is of particular interest concerning metal chelation therapy. In such a therapy, chelators should have an intermediate affinity, capable of disrupting low-affinity but pathologically relevant metal−Aβ interactions, without disrupting higher affinity essential metal−protein/peptide interactions. This allows specific, rather than systemic, chelation of excess metals in the brain of AD patients.

The dissociation constant of Zn−Aβ found in the literature differed depending on the conditions and methods used. Initially a substoichiometric binding of Zn to Aβ40 with a K_d of ~100 nM and a second site of 5 μM by using a displacement assay with radioactive and cold Zn binding to blotted Aβ40 has been reported (*17*). In a subsequent study also using blotted peptide, Clements et al. found no evidence for a submicromolar binding but confirmed a K_d of ~5 μM for Aβ40 by their value of 3.2 μM (*35*). Similar values in the low micromolar range (i.e., 5−10 μM) have also been reported for truncated Aβ (Aβ16) by competition with the Zn sensor zincon (*28*) and for Aβ28 by competition with Cu binding followed by fluorescence (~7 μM) (*34*). By using fluorescence enhancement of the single Tyr10 due to Zn binding to Aβ, different results have been reported (although under very similar conditions, Tris buffer, pH 7.4, 100−150 mM NaCl). Ricchelli et al. agreed with a K_d in the low micromolar range for Aβ16/40/42 (*36*), but Garzon et al. deduced a higher K_d of 300 μM for Aβ40 and 57 μM for Aβ42 (*37*). Although generally the apparent K_d of Aβ and its truncated forms Aβ16/28 is in the low micromolar range, not much is known of the influence of the aggregation state on $K_{d,app}$, a parameter which could explain some of the discrepancy reported.

In the present study we investigated the interaction of Zn with Aβ40 and Aβ42 as well as the truncated forms Aβ16 and Aβ28. Isothermal titration calorimetry and competition experiments with Zn sensors were applied to study this interaction. In particular, the apparent dissociation constants ($K_{d,app}$) were compared between soluble, aggregated Zn−Aβ40 and Aβ40 fibrils. This could have importance concerning metal chelation therapy, which is discussed.

MATERIALS AND METHODS

Materials. The peptides Aβ16, Aβ28, Aβ40, and Aβ42 were purchased from EZBiolab (Westfield, IN), Geneshere Biotechnologies (Paris, France), or Activotec (Cambridge, U.K.). The peptide concentrations were determined by absorption spectroscopy, by using the well-established extinction coefficient of Tyr at 275 nm, $\epsilon = 1410\ M^{-1}\ cm^{-1}$. A$\beta$40/42, which are prone to aggregation, were monomerized by a short incubation at pH 11−12 (*38*, *39*).

Aggregating Concentration. To determine at which concentration the different Aβ peptides aggregate in the presence of Zn, turbidity measurements at 400 nm were performed at different concentrations over 3 h (maximal time of an isothermal titration calorimetry (ITC) experiment). The results showed that Zn−Aβ16 is mainly soluble up to 60 μM, Zn−Aβ28 up to 20 μM, and Aβ40 up to 10 μM.

Isothermal Titration Calorimetry. ITC experiments were performed at 298.0 ± 0.1 K on a Microcal VP-ITC calorimeter (Microcal, Northampton, MA). Ligand and receptor solutions were prepared with the same buffer stock solution, 20 mM {2-(4-(2-hydroxyethyl)-1-piperazinyl)ethanesulfonic acid (HEPES), tris(hydroxymethyl)aminomethane (Tris), or cacodylate buffer with 100 mM NaCl at pH 7.4. All samples were degassed by being stirred under vacuum before use. In the cell, the peptide solution has a concentration of 10−140 μM. In each ITC experiment, about 30 injections of 7−8 μL of 150−800 μM zinc solution were made into the cell containing the peptide. The syringe speed was set at 300 rpm. Control experiments (heat dilution measurement) were performed by injecting zinc solution into the buffer, suggesting that the heat dilution was negligible for Tris buffer ($\Delta H_{Tris} \approx -0.15$ kcal.mol^{-1}). In the case of HEPES and cacodylate the ΔH of dilution was lower, but compared to the measured ΔH not insignificant (however, fits of the curve showed similar $K_{d,app}$ values independent of whether the dilution curve was subtracted). Thus, the ITC data were corrected for the heat of dilution of the titrant by subtracting the excess heats at high molar ratios of zinc to peptide. Some inverse titrations (100 μM Aβ16 solution injected into 500 μM zinc solution) confirmed the range of the reaction enthalpy values. Data were analyzed with Microcal Origin 7.0, and the fitting curves were calculated according to one set of the binding site model. The number of protons n_{H^+} released (>0) or taken up (<0) by the buffer during Zn−Aβ complexation is expressed by the following equation:

$$\Delta H_{binding} = \Delta H_{reaction} + n_{H^+}\Delta H_{ionization}$$

where $\Delta H_{binding}$ is the measured enthalpy of binding and $\Delta H_{reaction}$ the intrinsic enthalpy of reaction (*40*).

Apparent Dissociation Constant ($K_{d,app}$). The apparent Zn−Aβ dissociation constant was estimated by competition assay with the colorimetric Zn chelator zincon (2-carboxy-2′-hydroxy-5′-(sulfoformazyl)benzene) from Acros organics. It has been reported in the literature that zincon forms a complex with Zn^{II} in a 1:1 stoichiometry (Zn^{II}−zincon), showing a distinct absorption band at 620 nm ($\epsilon = 23200\ M^{-1}\ cm^{-1}$) at pH 7.4 and having an apparent binding constant (K_{app}) of 7.9×10^4, i.e., $K_{d,app}$ of 12.6 μM (*41*). We verified these parameters by titration of $ZnSO_4$ with different concentrations of zincon (10−20 μm) under our conditions (pH 7.4, 20 mM HEPES, 100 mM NaCl). Slighlty higher affinity was found ($K_{d,app}$ of 5.8 ± 1.5 μM), and the molecular extinction coefficient was lower than reported (15000 ± 1500 $M^{-1}\ cm^{-1}$).

The binding equilibrium of Zn^{II} between Aβ and zincon can be expressed as eq 1. The apparent binding constant of

$$Zn^{II}-A\beta + \text{zincon} \rightleftarrows A\beta + Zn^{II}-\text{zincon} \quad (1)$$

$Zn^{II}-A\beta$ can be calculated by solving eq 2 (Zi = zincon). In the case of titration of the Aβ−Zn complex with zincon, the absorption band at 620 nm is due to the Zn−zincon

$$\frac{[Zn^{II}-A\beta][Zi]}{[A\beta][Zn^{II}-Zi]} = \frac{K_{app(Zn-A\beta)}}{K_{app(Zn-Zi)}} \quad (2)$$

complex, which increases upon addition of zincon. The tailing from the absorption band at 470 nm due to apo-zincon was subtracted from the Zn−zincon complex signal. Assuming that all the zinc is bound, to either zincon or Aβ, it can be deduced that, at half-maximal absorption (see Figure 4), [zincon−Zn] = [Aβ−Zn] = $[Zn]_{total}/2$. [zincon] and [Aβ] could be calculated by subtracting the Zn-bound fraction from the initial concentration (i.e., $[zincon] = [zincon]_{total} - [Zn-zincon]$ and $[A\beta] = [A\beta]_{total} - [Zn-A\beta]$). Then, using the binding constant of Zn^{II}−zincon obtained from the titration realized the same day, the apparent binding constant of $Zn^{II}-A\beta$ could be calculated (*28*). To make sure that most Zn was bound to the ligand, an excess of Aβ over Zn (2:1 ratio) was used as a starting point of the titration. An analogous approach was used for the inverse titration, that is, the addition of Aβ to Zn−zincon. Both approaches yielded similar apparent binding constants of $Zn^{II}-A\beta$, indicating that reaction 1 had reached equilibrium.

A similar approach has been used with the fluorescent sensor Newport Green DCF dipotassium salt (NG) from Invitrogen (λ_{ex} = 485 nm, λ_{em} = 530 nm) (*42*). Its dissociation constant with zinc has been reported to be around 1 μM (*43*), which was confirmed by our experiments ((0.9 ± 0.5) × 10^6 M^{-1}). A concentration of 3 μM has been used in the titration experiment since the enhancement of fluorescence of the NG−Zn complex has been found to be linear with its concentration only up to 5 μM.

Zinquin (2-methyl-8-[(4-methylphenyl)sulfanylamino]-6-(carboxymethyloxy)quinoline, was purchased from Sigma-Aldrich. The excitation and emission wavelengths were 370 and 490 nm, respectively. Zinquin was first solubilized in DMSO and then in water. The concentration has been determined using the molecular extinction coefficient of about 9000 M^{-1} cm^{-1} at 340 nm calculated from ref *44*.

Fibril Preparation. A solution of 200 μM soluble Aβ40 in either Tris or HEPES (20 mM), NaCl (100 mM), and 0.01% NaN_3 at pH 7.4 was placed at 30 °C under gentle agitation for 3 weeks. The presence of fibrils was confirmed by negative stain transmission electron microscopy and ThT fluorescence (*45*).

RESULTS

Isothermal Titration Calorimetry. Isothermal titration calorimetry experiments can be used to study the binding between two molecules (often called the ligand and receptor) (*46*−*48*). Direct indications of three parameters can be obtained. These are the stoichiometry between the ligand and receptor, the binding constant (*K*), and the enthalpy (ΔH). On the basis of the binding constant and the enthalpy, the entropy (ΔS) can be calculated. However, it is important to note that the heat measured, and as a consequence the thermodynamic parameters (*K* and ΔH), stems from the entire reaction (i.e., from the starting reagents to the final product) and is thus apparent (for more detailed discussion of ITC measurement of metal−peptide/protein see refs *49*−*54*).

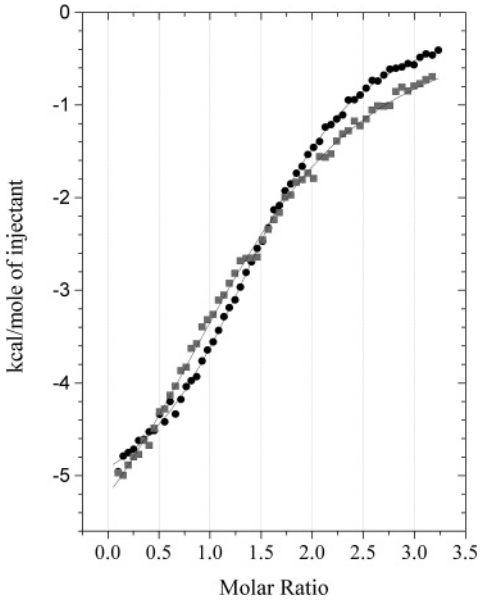

FIGURE 1: ITC: Zn titration to Aβ16 (■) and Aβ28 (●) at 140 μM in 20 mM Tris buffer, 100 mM NaCl, pH 7.4.

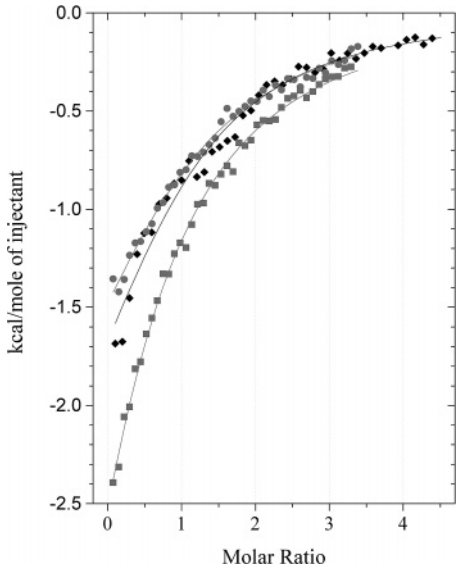

FIGURE 2: ITC of Aβ16 (■), Aβ28 (●), and Aβ40 (◆) at low concentration (10−20 μM) in 20 mM Tris buffer, 100 mM NaCl, pH 7.4.

As the K_d of Zn−Aβ16 has been reported to be in the low micromolar range, the first ITC measurements were conducted with the recommended 10−100 times higher concentration. An ITC measurement of Zn added to 140 μM Aβ16 or Aβ28 in 100 mM Tris/HCl at pH 7.4 is shown in Figure 1. The best fits at this concentration revealed apparent K_d values of 61 ± 4 and 30 ± 4 μM for Aβ16 and 28, respectively, but they also revealed a stoichiometry around 1.5, which is above the integer stoichiometry of the Zn-binding sites as suggested by spectroscopic data (*28*, *29*, *33*, *34*). Moreover, parallel turbidity measurement revealed that under this concentration Aβ28 and also partially Aβ16

Table 1: Apparent K_d (μM) Deduced from ITC[a]

	Aβ16	Aβ28	Aβ40
low concentration of Zn−Aβ (10−20 μM)	22 ± 15	10 ± 8	7 ± 3
high concentration of Zn−Aβ (70−150 μM)	71 ± 5[b]	30 ± 4[b]	3 ± 2
preformed fibrils of Aβ (without Zn)			9 ± 4

[a] Variance of the $K_{d,app}$ values indicated derived from the variance of the $K_{d,app}$ obtained by fitting several experiments under the same conditions. [b] The best fit yielded a stoichiometry of about 1.5.

aggregate in the presence of Zn over a time period of 3 h (time for the ITC experiment; for details see the Materials and Methods). This means that the measured heat is the sum of two events, i.e., sum of Zn binding to the peptide and the aggregation. To obtain only the contribution of Zn binding, ITC measurements at lower concentrations of 10−20 μM Aβ16/28 were conducted. Turbidity and centrifugation measurements showed that at this concentration Zn−Aβ16/28 did not aggregate significantly. The best fit of Zn titrations to Aβ16 and Aβ28 at lower concentration revealed generally an integer stoichiometry, i.e., one Zn per Aβ16/28. The $K_{d,app}$ values obtained for Aβ16 and Aβ28 were 22 ± 14 and 10 ± 8 μM, respectively (Table 1). However, at lower concentration the titration curve is only partially measured, and hence, the value obtained for ΔH is less accurate. As shown below, we confirmed ΔH by inverse titration, where it is much better defined.

After these experiments with the truncated peptides Aβ16 and Aβ28, measurements were extended to the full-length Aβ40. ITC experiments with Aβ40 were conducted at higher (70 μM) and lower (10 μM) concentration, i.e., under conditions where aggregation with Zn occurs or is almost absent. In either case the best fits exhibited an about 1:1 stoichiometry. The $K_{d,app}$ values were in the same range: 20 ± 14 and 7 ± 3 μM at high and low concentration, respectively (Table 1). Taken together the ITC experiments indicate that the $K_{d,app}$ values of Zn to Aβ40 and truncated peptides Aβ16/28 are in the low micromolar range. It seems that the longer peptides bind Zn slightly stronger than the shorter peptides, i.e., Aβ40 > Aβ28 > Aβ16. Moreover, Zn binding under aggregating and nonaggregating concentrations did not show a large difference, indicating that the aggregation does not contribute much to the measured reaction heat.

The same experiments have been repeated in the presence of HEPES and cacodylate buffer at pH 7.4 (100 mM NaCl). The results in HEPES confirmed the about 1:1 stoichiometry and a $K_{d,app}$ in the low micromolar range obtained in the Tris buffer. In the cacodylate buffer the signal was positive (ΔH > 0) but very small. The best fits revealed $K_{d,app}$ in the same range as in the other buffers Tris and HEPES. However, the stoichiometry given by the best fit was beyond a 1:1 complex.

The ITC measurement of Zn titration to Aβ in different buffers allows the estimation of the number of protons displaced by the binding of Zn^{II} to Aβ. The displaced proton will bind to the buffers, which have different ΔH values for proton binding. A difference in ΔH of two titrations, which differ only in their buffer, should only be due to the proton binding to the buffer. Since the ΔH values of Tris, HEPES, and cacodylate are known (11.51, 5.0, and −0.56 kcal/mol, respectively) (*55*), the number of protons displaced by Zn binding has been calculated to be 0.76 ± 0.37 from the ITC measurements (Figure 3).

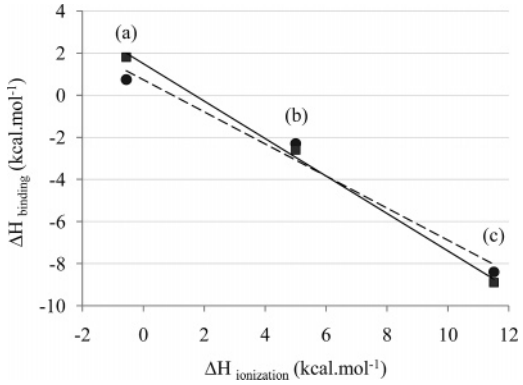

FIGURE 3: Enthalpy change of binding of Aβ16 to zinc at pH 7.4 as a function of the ionization enthalpy of the reaction buffer (a, cacodylate; b, HEPES; c, Tris). The absolute value of the slope of the linear regression yields the number of protons released by the buffer when one zinc binds to one Aβ16. The circles correspond to the values obtained when Zn was added (0.76 ± 0.37 proton released) and the squares when the peptide was added (0.89 ± 0.07 proton released).

Due to the relatively low concentrations of Aβ in the ITC measurements, the ΔH deduced from the binding isotherm is not that well defined. This is due to the fact that when Zn is added at low Aβ concentration, Zn is in equilibrium between free and bound. To get a good estimate of the ΔH of Zn binding to Aβ, conditions are needed where Zn completely binds to Aβ. This is achieved by an inverse experiment, when clearly substoichiometric amounts of Aβ are added to Zn in the buffer. Under these conditions, all Aβ added will bind to Zn and ΔH is better defined. Such experiments were conducted in Tris, HEPES, and cacodylate and revealed ΔH values of −8.9, −2.6, and +1.8 kcal/mol, respectively. This corresponds to a replacement of 0.89 ± 0.07 proton, hence confirming, with more accuracy, the previous value of 0.8 proton displaced by Zn binding to Aβ. Moreover, the values for ΔH obtained by the inverse experiment in Tris and HEPES buffers are very similar to the ΔH values obtained by the fit of the titration curve from titration of Zn to the peptides and hence corroborate the other parameters of the fit, i.e., $K_{d,app}$ and stoichiometry (see above).

Determination of $K_{d,app}$ of Zn Binding to Soluble Aβ by Competition Assay Followed by Absorption and Fluorescence Spectroscopy. To confirm the above measured $K_{d,app}$ of Zn−Aβ and to have the possibility to measure at lower peptide concentration and thus under nonaggregating conditions, $K_{d,app}$ was also measured by a competition assay. The apparent binding constants can be estimated by competition with a chelator, for which the binding constant is known and is in the same range. The Zn chelator zincon has been shown to be appropriate for Zn−protein complexes (*41*, *56*, *57*) and was already successfully applied for the soluble Aβ16 (*28*). Thus, the same methodology was applied to measure the $K_{d,app}$ of Aβ28, Aβ40, and Aβ42 at a concentration where insignificant aggregation was observed by turbidity (i.e., at 10 μM). Figure 4 shows the titration experiments (see the Material and Methods) followed by absorption at 620 nm. The upper panel shows the absorption at 620 nm of the Zn−zincon complex by adding increasing amounts of Aβ40. The decrease of the absorption at 620 nm reflected

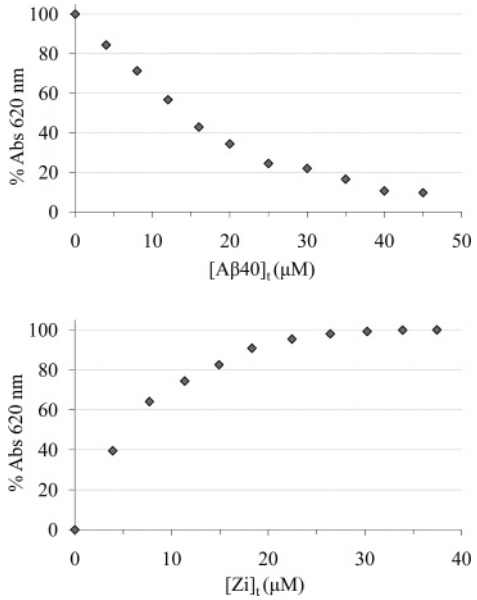

FIGURE 4: Estimation of the Zn^{II} binding constant by competition with the chelator zincon. Upper panel: Absorption at 620 nm of the Zn−zincon complex upon addition of increasing amounts of Aβ1−40. Conditions: 10 μM zincon, 5 μM Zn, pH 7.4, 20 mM HEPES, 100 mM NaCl. Lower panel: To the complex of Zn−Aβ1−40 were added increasing concentrations of zincon, and the absorption at 620 nm of Zn−zincon was followed. Conditions: 10 μM Aβ1−40, 50 μM Zn, pH 7.4, 20 mM HEPES, 100 mM NaCl. The ordinate is the percent absorption at 620 nm, with 100% standing for the maximum absorption obtained (at t_0 and t_∞, respectively).

Table 2: Apparent K_d from Zincon (Zi Added, [Aβ]/[Zn] = 2)

peptide	$K_{d,app}$ (μM)
Aβ16, nonaggretated	14 ± 5
Aβ28, nonaggregated	12 ± 5
Aβ40 and Aβ42, nonaggregated	7 ± 3
Aβ40, fibrils	9 ± 6
Aβ40 or Aβ42 + Zn, aggregated for 3 h	3 ± 2

the transfer of Zn from zincon to Aβ40. About 13 μM Aβ40 was necessary to decrease the band at 620 nm by half, indicating that half of the 5 μM Zn bound to zincon was transferred to Aβ40. Thus, globally the binding constants were very similar, whereas zincon was slightly stronger than Aβ40. The calculations lead to a $K_{d,app}$ of about 6.3 μM for Zn−Aβ40. The lower panel shows the inverse experiment, in which zincon was added to Zn−Aβ40. Here half of the 5 μM Zn was bound to zincon after addition of 6 μM zincon (thus, $K_{d,app} \approx 9.6$ μM). This confirmed the above experiment which showed that globally the binding constants were in the same range, zincon being a little stronger then Aβ40. The fact that the two approaches yielded the same $K_{d,app}$ (within experimental limits) indicated that the reaction of Zn exchange reached equilibrium, a prerequisite for the calculation of $K_{d,app}$.

Analogue experiments were conducted with Aβ42, Aβ28, and Aβ16 (Table 2). In general, no large difference between the entire and truncated peptide was observed at low concentration. The $K_{d,app}$ values were in the low micromolar range (1−20 μM), with a tendency to a higher affinity by the longer peptides. Similar experiments were performed with the Zn-sensitive chelator Newport Green. Newport Green has an apparent K_d of 1 μM (*42*, *43*, *58*). This value was confirmed by Zn titration to Newport Green under our conditions (20 mM HEPES buffer, pH 7.4, 100 mM NaCl), which revealed a $K_{d,app}$ of about 0.9 μM. In general, the competition experiments confirmed a $K_{d,app}$ in the low micromolar range for Zn−Aβ. Also the tendency that the longer Aβ peptides bind Zn slightly stronger was observed again.

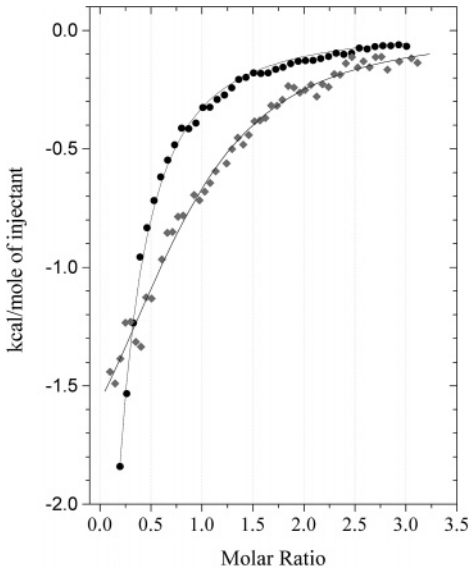

FIGURE 5: ITC of Zn titration to soluble Aβ40 (70 μM) (◆) and to fibrils of Aβ40 (60 μM) (●) in 20 mM Tris buffer, 100 mM NaCl, pH 7.4.

Another widely used fluorescent Zn chelator is zinquin. Zinquin has an apparent binding affinity at physiological pH in the picomolar to low nanomolar range, i.e., much stronger than that of soluble Zn−Aβ (*44*). A titration experiment of zinquin to Zn−Aβ showed that zinquin withdraws Zn quantitatively from Aβ. In contrast, Aβ was not able to compete significantly for Zn binding with zinquin, even at a 10 times excess of Aβ compared to zinquin. These results are in line with the at least 100 times stronger affinity of zinquin compared to Aβ.

Zn Binding to Preformed Fibrils of Aβ. Next, Zn binding to Aβ40 fibrils (incubated over 3 weeks in the absence of Zn) was measured. The ITC measurement is shown in Figure 5. The best fits revealed a $K_{d,app}$ of 9 ± 4 μM, i.e., not significantly different from that of Zn binding to soluble Aβ (Table 1). Also ΔH did not differ significantly. However, a change was observed concerning the stoichiometry of the Zn-binding site, i.e., a substoichiometric binding of ~0.2 equiv of Zn per Aβ peptide (when using 60 μM fibrils). This suggests that Zn binds to only a portion of the binding sites with similar $K_{d,app}$ values. This could indicate that the binding site is perhaps the same. The rest of the binding sites either are not accessible to Zn binding because they are buried in the fibril structure or did change due to structural modifications induced by aggregation. Such changes could lead to a lower affinity not detectable by ITC or to Zn binding with a very small ΔH not detectable by ITC. To confirm these results, Zn binding to the fibrils was also analyzed by the competition assay with zincon, which was in agreement with substoichiometric Zn binding with a $K_{d,app}$ in the low micromolar range (not shown) (Table 2).

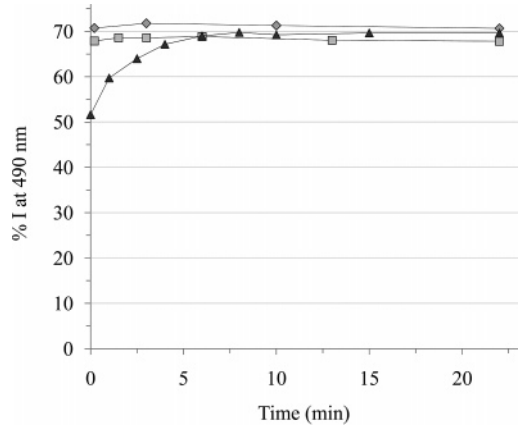

FIGURE 6: Fluorescence relative intensity of a solution of 2.1 equiv of zinquin with 60 μM zinc (◇), Aβ16−Zn (□), or Aβ40−Zn, incubated overnight (▲).

Zn Binding in Zn-Induced Aggregates of Aβ. Zn binding to Aβ induces rapid aggregation and formation of Zn−Aβ aggregates. To measure the apparent binding affinity of Zn in these aggregates, they were titrated with the Zn sensors zinquin and zincon.[2] First, the question was addressed of whether Zn in the Zn−Aβ aggregates is readily accessible to chelator binding. As zinquin has a much stronger (at least 100 times) apparent Zn-binding affinity than the soluble Zn−Aβ, all Zn should be transferred to zinquin. Indeed, Figure 6 shows that zinquin immediately binds free Zn and Zn from the soluble Zn−Aβ16 quantitatively after mixing (i.e., in a couple of seconds). Addition of zinquin to Zn−Aβ40 aggregates yielded a complete Zn transfer from the Zn−Aβ aggregates to zinquin. However, in this case the transfer was only completed after 5 min. This indicates that Zn transfer to zinquin is slower in Zn−Aβ aggregates than in soluble Zn−Aβ. Moreover, it also shows that zinquin has a stronger affinity than Zn−Aβ aggregates, which limits the $K_{d,app}$ of Zn in Zn−Aβ aggregates to a value in the nanomolar range or above. To get a better estimate of the binding affinity of Zn−Aβ aggregates, the chelators zincon and Newport Green were used. Competition experiments with zincon or Newport Green suggested a small but reproducible 2−3-fold stronger Zn binding to the Zn-induced aggregates of Aβ28 and Aβ40 compared to soluble Aβ28/Aβ40.[3]

DISCUSSION

The present results indicate the $K_{d,app}$ values of Zn binding (pH 7.4, 0.1 M NaCl) of different Aβ forms are relatively similar, i.e., all in the low micromolar range (3−15 μM). No indication was found for the initially reported high-affinity binding site (K_d of 104 nM) (*17*), but the present $K_{d,app}$ agrees with values reported for truncated, soluble Aβ16/28 (*28*, *29*, *34*). No significant difference was observed at nonaggregating and aggregating concentrations. This includes Zn-induced Aβ40 aggregates as well as Zn binding to fibrils formed in the absence of Zn. This suggests that the affinity of the Zn-binding site is similar in the soluble and the different aggregated forms. Thus, it is very possible that the Zn-binding site is the same in aggregated and nonaggregated Aβ including the same ligands (three His residues, Asp1, or Glu11).[4]

Although no significant difference in Zn affinity between soluble and aggregated Aβ could be observed, other parameters showed differences. First, in the case of the Zn-induced Aβ aggregates, the kinetics of Zn transfer from the aggregate to the zinc sensor was substantially slower. Two scenarios could explain this slower kinetics: (i) The Zn sites are buried in the aggregate, and hence, it takes more time to transfer zinc to the sensor. (ii) As the aggregates are normally in equilibrium with soluble Aβ (*59*, *60*), the sensor withdraws Zn rapidly from the soluble fraction but more slowly or not at all from the aggregates. This provokes resolubilization of Zn−Aβ from the aggregates to reach equilibrium of soluble and aggregated Zn−Aβ. In this case the kinetics would reflect the resolubilization of the Zn−Aβ aggregates. The second remarkable difference was observed between Zn binding to soluble Aβ and that to preformed Aβ fibrils. Soluble Aβ bound about 1 equiv of Zn, the preformed fibrils bound only a substoichiometric (i.e., ~0.2 equiv) amount of Zn, indicating that not all binding sites were accessible (or existing).

The finding that the $K_{d,app}$ of Zn to Aβ is in the low micromolar range independent of its aggregation state has implications for the so-called metal chelation therapy. The concept of this therapy consists of chelating the metal ions bound to Aβ, and it favors disaggregation from toxic aggregate forms (e.g., oligomers) to nontoxic monomers. Several chelators of this type have been developed or have entered clinical trials, such as clioquinol (*12*), DP-109 (*13*), and a bifunctional metal chelator (*61*). Such chelators should have an intermediate affinity, capable of disrupting low-affinity but pathologically relevant metal−Aβ interactions, but do not withdraw higher affinity essential metal−protein/peptide interactions. This allows specific, rather than systemic, chelation of excess metals in the brain of AD patients. The K_d of clioquinol at pH 7.4 has been determined (*62*). An apparent K_d value of 1.4×10^{-9} M has been reported at concentrations of 1 μM Zn and 200 μM clioquinol. However, since clioquinol forms a 2:1 complex with Zn (*63*), the apparent K_d is dependent on the clioquinol concentration, for which 200 μM is rather high for physiological conditions. A K_d of 4×10^{-8} M (pH 7.0) was determined for Zn−DP-109 (Jonathan Friedman, personal communication). Our results indicate that, concerning Zn, a $K_{d,app}$ of about 1 μM

[2] The opposite titration, i.e., addition of Zn−Aβ aggregates to the zinc sensor, was avoided, because in such an experiment Zn−Aβ aggregates would be highly diluted into the sensor solution, with the risk of disaggregation of the Zn−Aβ aggregates.

[3] The observation that the capacity of zincon or Newport Green to withdraw Zn from Zn−Aβ aggregates is smaller than from soluble Zn−Aβ is assigned to a higher affinity of Zn in the aggregates (thermodynamics) and not kinetics, because (i) the experiments with zinquin (see above) showed that Zn transfer is finished after a couple of minutes and (ii) the reaction of addition of zincon and Newport Green to Zn−Aβ was followed for over 10 min and no increase in the absorption band at 620 nm (reflecting the Zn−zincon complex) or fluorescence of Zn−Newport Green was observed (such experiments are limited to the minute time scale since the Zn−zincon and −Newport Green complexes degrade slowly with time).

[4] Supposing that the Zn-binding site is the same in the soluble monomeric and aggregated Aβ would point more to a mechanism where Zn binds to Aβ as a monomeric complex and induces a conformational change, which favors the aggregation by pure peptide−peptide contacts. It points less to a mechanism where Zn−Aβ is first a soluble monomeric complex and aggregation is induced by Zn forming a bridge between two molecules of Aβ, because this would include a change in the coordination (for discussion of the two mechanisms see ref *18*.

is enough to withdraw the majority of the Zn from Aβ, independent of the aggregation state. Moreover, a chelator with a K_d in this range is unlikely to withdraw Zn from proteins and enzymes as they have generally a stronger Zn affinity (*64*−*66*).

ITC Proton Displacement. ITC measurement indicated that Zn binding to Aβ leads to the release of 0.8−0.9 proton. It is known from the literature that Zn binds to three His residues. As a fourth ligand, aspartate at position 1, either by the N-terminus or carboxylate side chain, is the most reported (*28*, *29*, *34*). However, the carboxylate of Glu11 has also been suggested (*31*). As Asp and Glu are normally deprotonated at pH 7.4, Zn binding does not lead to proton release. In contrast, the pK_a of the N-terminus of a peptide is normally around 7.8, a value confirmed by 8.0 deduced from potentiometric measurements (*67*). Thus, Zn binding to the N-terminus would lead to a release of 0.8 proton at pH 7.4. This would in principle allow the distinction between Zn binding to a carboxylate and that to the N-terminus, if the pK_a of the three His residues are known as well. Unfortunately, two quite different sets of data are available for pK_a of His 6, 13, and 14. NMR measurements on acetylated Aβ16 determined pK_a values of 7.0, 6.9, and 6.8, respectively. Potentiometric measurement suggested pK_a values of 7.0, 6.5, and 5.7 for nonacetylated Aβ16. On the basis of the NMR data, the calculation gives 0.7 ± 0.3 proton released by Zn binding to the three His residues, in agreement with our measurement. When N-terminal binding is added, 1.5 ± 0.4 protons are calculated to be released, which is not in agreement with the data. For the potentiometric set, Zn binding to only three His residues gives 0.4 ± 0.3 proton replaced, when including the N-terminus as a ligand, 1.2 ± 0.4 protons. Therefore, these pK_a values deduced from potentiometry are more in favor of Zn binding to the N-terminus. However, in our previous paper (*28*), we found chemical shifts of the three His residues at different pH for the nonacetylated Aβ16 almost identical to those reported for the acetylated Aβ16, indicating that under our conditions the pK_a of the three His residues corresponds to 6.9 ± 0.1. Thus, it seems that the measured release of 0.89 proton by Zn binding to Aβ is entirely due to the binding to the three His residues. This suggests that no other proton is released, which is in favor of binding to a carboxylate rather than the N-terminus (or tyrosine).[5]

ITC Comparison between Cu and Zn. We previously reported ITC measurement on the interaction of Cu^{2+} with Aβ16 and Aβ28 (*53*). Cu is supposed to bind to the same three His residues as Zn in a square planar geometry. The fourth ligand is likely to be Asp1 (by either the N-terminus and carboxylate). Cu binding was stronger than Zn binding, and it was more dependent on the buffer (see Table 1). In HEPES the $K_{d,app}$ of Cu was ~0.1 μM compared to ~10 μM for Zn, whereas in Tris the $K_{d,app}$ of Cu was only ~1 μM. Not only were the $K_{d,app}$ values different, so were the ΔH and ΔS values (Table 3). In the case of Zn binding ΔS, even if not very accurate, was clearly smaller than for Cu binding. The difference in ΔH was less striking, but Zn binding had a little more negative ΔH. This means that for Zn binding the enthalpic contribution is slightly higher and the entropic lower compared to those for Cu binding. In other words, it is principally the higher entropic contribution which is responsible for the higher affinity of Aβ toward Cu (compared to Zn). The higher entropic contribution could be due to (i) release of more water molecules from the hydrated Cu^{II} upon Cu^{II}−Aβ formation, (ii) release of more water molecules from the peptide hydration, (iii) conformational changes, i.e., fewer degrees of freedom upon binding of Cu^{II}, or (iv) entropic changes due to metal−buffer interaction (before complex formation). In particular, assumption i is likely to contribute to the higher entropic contribution of Cu versus Zn binding. Hydrated Cu is likely to lose all its water upon binding to Aβ, since no indication for a labile ligand to the square planar Cu in Cu−Aβ was found (*53*). In contrast, Zn, which is most likely bound to the same four amino acids, prefers penta- and hexacoordination and is thus likely to keep one or two water molecules upon binding to Aβ. This is supported by the ~13−20 cal $mol^{-1}K^{-1}$ higher value of ΔS for Cu than Zn binding (see Table 3) and by the fact that a value of 9.5 cal $mol^{-1}K^{-1}$ per water released from a metal ion has been reported (*52*).

Table 3: Comparison of the Thermodynamic Parameters, Obtained by ITC, of the Zn−Aβ16 and Cu−Aβ16 Interactions

metal	K_d (μM)	ΔH_{Tris} (kcal mol^{-1})	ΔS_{Tris} (cal mol^{-1})	ΔH_{HEPES} (kcal mol^{-1})	ΔS_{HEPES} (cal mol^{-1})
Zn^{II}	22 ± 15	-8.4 ± 4.0	-8 ± 15	-2.3 ± 0.2	18 ± 7
Cu^{II}	0.1	−3	12	−0.5	31

CONCLUSIONS

In conclusion, the present work shows evidence that the apparent Zn-binding affinity to Aβ40 and Aβ42 is in the low micromolar range and is not very dependent on the aggregation state of Aβ, i.e., soluble Aβ, Aβ fibrils, or Zn-induced Aβ. Moreover, Zn in the soluble or aggregated Zn−Aβ form is well accessible for Zn chelators. This suggests that chelators, i.e., in metal chelation therapy, withdraw Zn concomitantly from soluble and aggregated Zn−Aβ, and specific chelation only from soluble Zn−Aβ seems very difficult.

ACKNOWLEDGMENT

We thank Dr. D. Fournier (IPBS, Toulouse) for access to the microcalorimeter.

REFERENCES

1. Suh, Y. H., and Checler, F. (2002) Amyloid precursor protein, presenilins, and alpha-synuclein: molecular pathogenesis and pharmacological applications in Alzheimer's disease, *Pharmacol. Rev. 54*, 469−525.
2. Hardy, J., and Selkoe, D. J. (2002) The amyloid hypothesis of Alzheimer's disease: progress and problems on the road to therapeutics, *Science 297*, 353−356.
3. Klein, W. L., Stine, W. B., Jr., and Teplow, D. B. (2004) Small assemblies of unmodified amyloid beta-protein are the proximate neurotoxin in Alzheimer's disease, *Neurobiol. Aging 25*, 569−580.
4. Multhaup, G., and Masters, C. L. (1999) Metal binding and radical generation of proteins in human neurological diseases and aging, *Met. Ions Biol. Syst. 36*, 365−387.

[5] The suggestion that Zn does not bind predominantly to the N-terminus is not in contradiction with the NMR measurements, which showed a line broadening of the resonances of the N-terminal Asp upon Zn binding. Transient and partial Zn binding could be sufficient to explain the line broadening in NMR, but would not lead to substantial proton release in ITC.

5. Bush, A. I., Pettingell, W. H., Multhaup, G., d Paradis, M., Vonsattel, J. P., Gusella, J. F., Beyreuther, K., Masters, C. L., and Tanzi, R. E. (1994) Rapid induction of Alzheimer A beta amyloid formation by zinc, *Science 265*, 1464−1467.
6. Selkoe, D. J. (2001) Alzheimer's disease: genes, proteins, and therapy, *Physiol. Rev. 81*, 741−766.
7. Bush, A. I. (2003) The metallobiology of Alzheimer's disease, *Trends Neurosci. 26*, 207−214.
8. Cherny, R. A., Legg, J. T., McLean, C. A., Fairlie, D. P., Huang, X., Atwood, C. S., Beyreuther, K., Tanzi, R. E., Masters, C. L., and Bush, A. I. (1999) Aqueous dissolution of Alzheimer's disease Abeta amyloid deposits by biometal depletion, *J. Biol. Chem. 274*, 23223−23228.
9. Bush, A. I., Multhaup, G., Moir, R. D., Williamson, T. G., Small, D. H., Rumble, B., Pollwein, P., Beyreuther, K., and Masters, C. L. (1993) A novel zinc(II) binding site modulates the function of the beta A4 amyloid protein precursor of Alzheimer's disease, *J. Biol. Chem. 268*, 16109−16112.
10. Ciuculescu, E. D., Mekmouche, Y., and Faller, P. (2005) Metal-binding properties of the peptide APP170−188: a model of the ZnII-binding site of amyloid precursor protein (APP), *Chemistry 11*, 903−909.
11. Lee, J. Y., Cole, T. B., Palmiter, R. D., Suh, S. W., and Koh, J. Y. (2002) Contribution by synaptic zinc to the gender-disparate plaque formation in human Swedish mutant APP transgenic mice, *Proc. Natl. Acad. Sci. U.S.A. 99*, 7705−7710.
12. Cherny, R. A., Atwood, C. S., Xilinas, M. E., Gray, D. N., Jones, W. D., McLean, C. A., Barnham, K. J., Volitakis, I., Fraser, F. W., Kim, Y., Huang, X., Goldstein, L. E., Moir, R. D., Lim, J. T., Beyreuther, K., Zheng, H., Tanzi, R. E., Masters, C. L., and Bush, A. I. (2001) Treatment with a copper-zinc chelator markedly and rapidly inhibits beta-amyloid accumulation in Alzheimer's disease transgenic mice, *Neuron 30*, 665−676.
13. Lee, J. Y., Friedman, J. E., Angel, I., Kozak, A., and Koh, J. Y. (2004) The lipophilic metal chelator DP-109 reduces amyloid pathology in brains of human beta-amyloid precursor protein transgenic mice, *Neurobiol. Aging 25*, 1315−1321.
14. Adlard, P. A., and Bush, A. I. (2006) Metals and Alzheimer's disease, *J. Alzheimer's Dis. 10*, 145−163.
15. Boldron, C., Van der Auwera, I., Deraeve, C., Gornitzka, H., Wera, S., Pitie, M., Van Leuven, F., and Meunier, B. (2005) Preparation of cyclo-phen-type ligands: chelators of metal ions as potential therapeutic agents in the treatment of neurodegenerative diseases, *ChemBioChem 6*, 1976−1980.
16. Mantyh, P. W., Ghilardi, J. R., Rogers, S., DeMaster, E., Allen, C. J., Stimson, E. R., and Maggio, J. E. (1993) Aluminum, iron, and zinc ions promote aggregation of physiological concentrations of beta-amyloid peptide, *J. Neurochem. 61*, 1171−1174.
17. Bush, A. I., Pettingell, W. H., Jr., Paradis, M. D., and Tanzi, R. E. (1994) Modulation of A beta adhesiveness and secretase site cleavage by zinc, *J. Biol. Chem. 269*, 12152−12158.
18. Talmard, C., Guilloreau, L., Coppel, Y., Mazarguil, H., and Faller, P. (2007) Amyloid-beta peptide forms monomeric complexes with Cu(II) and Zn(II) prior to aggregation, *ChemBioChem 8*, 163−165.
19. Yang, D. S., McLaurin, J., Qin, K., Westaway, D., and Fraser, P. E. (2000) Examining the zinc binding site of the amyloid-beta peptide, *Eur. J. Biochem. 267*, 6692−6698.
20. Raman, B., Ban, T., Yamaguchi, K., Sakai, M., Kawai, T., Naiki, H., and Goto, Y. (2005) Metal ion-dependent effects of clioquinol on the fibril growth of an amyloid {beta} peptide, *J. Biol. Chem. 280*, 16157−16162.
21. Klug, G. M., Losic, D., Subasinghe, S. S., Aguilar, M. I., Martin, L. L., and Small, D. H. (2003) Beta-amyloid protein oligomers induced by metal ions and acid pH are distinct from those generated by slow spontaneous ageing at neutral Ph, *Eur. J. Biochem. 270*, 4282−4293.
22. Yoshiike, Y., Tanemura, K., Murayama, O., Akagi, T., Murayama, M., Sato, S., Sun, X., Tanaka, N., and Takashima, A. (2001) New insights on how metals disrupt amyloid beta-aggregation and their effects on amyloid-beta cytotoxicity, *J. Biol. Chem. 276*, 32293−32299.
23. House, E., Collingwood, J., Khan, A., Korchazkina, O., Berthon, G., and Exley, C. (2004) Aluminium, iron, zinc and copper influence the in vitro formation of amyloid fibrils of Abeta42 in a manner which may have consequences for metal chelation therapy in Alzheimer's disease, *J. Alzheimer's Dis. 6*, 291−301.
24. Liu, S. T., Howlett, G., and Barrow, C. J. (1999) Histidine-13 is a crucial residue in the zinc ion-induced aggregation of the A beta peptide of Alzheimer's disease, *Biochemistry 38*, 9373−9378.
25. Miura, T., Suzuki, K., Kohata, N., and Takeuchi, H. (2000) Metal binding modes of Alzheimer's amyloid beta-peptide in insoluble aggregates and soluble complexes, *Biochemistry 39*, 7024−7031.
26. Curtain, C. C., Ali, F., Volitakis, I., Cherny, R. A., Norton, R. S., Beyreuther, K., Barrow, C. J., Masters, C. L., Bush, A. I., and Barnham, K. J. (2001) Alzheimer's disease amyloid-beta binds copper and zinc to generate an allosterically ordered membrane-penetrating structure containing superoxide dismutase-like subunits, *J. Biol. Chem. 276*, 20466−20473.
27. Kozin, S. A., Zirah, S., Rebuffat, S., Hoa, G. H., and Debey, P. (2001) Zinc binding to Alzheimer's Abeta(1−16) peptide results in stable soluble complex, *Biochem. Biophys. Res. Commun. 285*, 959−964.
28. Mekmouche, Y., Coppel, Y., Hochgrafe, K., Guilloreau, L., Talmard, C., Mazarguil, H., and Faller, P. (2005) Characterization of the ZnII binding to the peptide amyloid-beta1−16 linked to Alzheimer's disease, *ChemBioChem 6*, 1663−1671.
29. Syme, C. D., and Viles, J. H. (2006) Solution 1H NMR investigation of Zn2+ and Cd2+ binding to amyloid-beta peptide (Abeta) of Alzheimer's disease, *Biochim. Biophys. Acta 1764*, 246−256.
30. Zirah, S., Rebuffat, S., Kozin, S. A., Debey, P., Fournier, F., Lesage, D., and Tabet, J.-C. (2003) Zinc binding properties of the amyloid fragment Ab(1−16) studied by electrospray-ionization mass spectrometry, *Int. J. Mass Spectrom. 228*, 999−1016.
31. Zirah, S., Kozin, S. A., Mazur, A. K., Blond, A., Cheminant, M., Segalas-Milazzo, I., Debey, P., and Rebuffat, S. (2006) Structural changes of region 1−16 of the Alzheimer disease amyloid beta-peptide upon zinc binding and in vitro aging, *J. Biol. Chem. 281*, 2151−2161.
32. Stellato, F., Menestrina, G., Serra, M. D., Potrich, C., Tomazzolli, R., Meyer-Klaucke, W., and Morante, S. (2006) Metal binding in amyloid beta-peptides shows intra- and inter-peptide coordination modes, *Eur. Biophys. J. 35*, 340−351.
33. Hou, L., and Zagorski, M. G. (2006) NMR reveals anomalous copper(II) binding to the amyloid Abeta peptide of Alzheimer's disease, *J. Am. Chem. Soc. 128*, 9260−9261.
34. Danielsson, J., Pierattelli, R., Banci, L., and Graslund, A. (2007) High-resolution NMR studies of the zinc-binding site of the Alzheimer's amyloid beta-peptide, *FEBS J. 274*, 46−59.
35. Clements, A., Allsop, D., Walsh, D. M., and Williams, C. H. (1996) Aggregation and metal-binding properties of mutant forms of the amyloid A beta peptide of Alzheimer's disease, *J. Neurochem. 66*, 740−747.
36. Ricchelli, F., Drago, D., Filippi, B., Tognon, G., and Zatta, P. (2005) Aluminum-triggered structural modifications and aggregation of beta-amyloids, *Cell. Mol. Life Sci. 62*, 1724−1733.
37. Garzon-Rodriguez, W., Yatsimirsky, A. K., and Glabe, C. G. (1999) Binding of Zn(II), Cu(II), and Fe(II) ions to Alzheimer's A beta peptide studied by fluorescence, *Bioorg. Med. Chem. Lett 9*, 2243−2248.
38. Hou, L., Shao, H., Zhang, Y., Li, H., Menon, N. K., Neuhaus, E. B., Brewer, J. M., Byeon, I. J., Ray, D. G., Vitek, M. P., Iwashita, T., Makula, R. A., Przybyla, A. B., and Zagorski, M. G. (2004) Solution NMR studies of the A beta(1−40) and A beta(1−42) peptides establish that the Met35 oxidation state affects the mechanism of amyloid formation, *J. Am. Chem. Soc. 126*, 1992−2005.
39. Fezoui, Y., Hartley, D. M., Harper, J. D., Khurana, R., Walsh, D. M., Condron, M. M., Selkoe, D. J., Lansbury, P. T., Jr., Fink, A. L., and Teplow, D. B. (2000) An improved method of preparing the amyloid beta-protein for fibrillogenesis and neurotoxicity experiments, *Amyloid 7*, 166−178.
40. Pierce, M. M., Raman, C. S., and Nall, B. T. (1999) Isothermal titration calorimetry of protein-protein interactions, *Methods 19*, 213−221.
41. Shaw, C. F., Laib, J. E., Sevas, M. M., and Petering, D. H. (1990), *Inorg. Chem. 29*, 403−408.
42. Lukowiak, B., Vandewalle, B., Riachy, R., Kerr-Conte, J., Gmyr, V., Belaich, S., Lefebvre, J., and Pattou, F. (2001) Identification and purification of functional human beta-cells by a new specific zinc-fluorescent probe, *J. Histochem. Cytochem. 49*, 519−528.
43. Jiang, P., and Gui, Z. (2004) Florescent detection of zinc in biological systems: recent develpoment on the design of chemosensors and biosensors, *Coord. Chem. Rev. 248*, 205−229.

44. Fahrni, C. J., and O'Halloran. (1999) Aqueous coordination chemistry of quinoline-based fluorescence probes for the biological chemistry of zinc, *J. Am. Chem. Soc. 121*, 11448−11458.
45. Nilsson, M. R. (2004) Techniques to study amyloid fibril formation in vitro, *Methods 34*, 151−160.
46. Ababou, A., and Ladbury, J. E. (2007) Survey of the year 2005: literature on applications of isothermal titration calorimetry, *J. Mol. Recognit. 20*, 4−14.
47. Privalov, P. L., and Dragan, A. I. (2007) Microcalorimetry of biological macromolecules, *Biophys. Chem. 126*, 16−24.
48. Ladbury, J. E. (2004) Application of isothermal titration calorimetry in the biological sciences: things are heating up!, *Biotechniques 37*, 885−887.
49. Atwood, C. S., Scarpa, R. C., Huang, X., Moir, R. D., Jones, W. D., Fairlie, D. P., Tanzi, R. E., and Bush, A. I. (2000) Characterization of copper interactions with alzheimer amyloid beta peptides: identification of an attomolar-affinity copper binding site on amyloid beta1−42, *J. Neurochem. 75*, 1219−1233.
50. Zhang, Y., and Wilcox, D. E. (2002) Thermodynamic and spectroscopic study of Cu(II) and Ni(II) binding to bovine serum albumin, *J. Biol. Inorg. Chem. 7*, 327−337.
51. Blasie, C. A., and Berg, J. M. (2002) Structure-based thermodynamic analysis of a coupled metal binding-protein folding reaction involving a zinc finger peptide, *Biochemistry 41*, 15068−15073.
52. Blasie, C. A., and Berg, J. M. (2003) Kinetics and thermodynamics of copper(II) binding to apoazurin, *J. Am. Chem. Soc. 125*, 6866−6867.
53. Guilloreau, L., Damian, L., Coppel, Y., Mazarguil, H., Winterhalter, M., and Faller, P. (2006) Structural and thermodynamical properties of CuII amyloid-beta16/28 complexes associated with Alzheimer's disease, *J. Biol. Inorg. Chem. 11*, 1024−1038.
54. Zhang, Y., Akilesh, S., and Wilcox, D. E. (2000) Isothermal titration calorimetry measurements of Ni(II) and Cu(II) binding to His, GlyGlyHis, HisGlyHis, and bovine serum albumin: a critical evaluation, *Inorg. Chem. 39*, 3057−3064.
55. Bradshaw, J. M., and Waksman, G. (1998) Calorimetric investigation of proton linkage by monitoring both the enthalpy and association constant of binding: application to the interaction of the Src SH2 domain with a high-affinity tyrosyl phosphopeptide, *Biochemistry 37*, 15400−15407.
56. Huang, M., Krepkiy, D., Hu, W., and Petering, D. H. (2004) Zn-, Cd-, and Pb-transcription factor IIIA: properties, DNA binding, and comparison with TFIIIA-finger 3 metal complexes, *J. Inorg. Biochem. 98*, 775−785.
57. Armas, A., Sonois, V., Mothes, E., Mazarguil, H., and Faller, P. (2006) Zinc(II) binds to the neuroprotective peptide humanin, *J. Inorg. Biochem. 100*, 1672−1678.
58. Thompson, R. B., Peterson, D., Mahoney, W., Cramer, M., Maliwal, B. P., Suh, S. W., Frederickson, C., Fierke, C., and Herman, P. (2002) Fluorescent zinc indicators for neurobiology, *J. Neurosci. Methods 118*, 63−75.
59. Wetzel, R. (2006) Kinetics and thermodynamics of amyloid fibril assembly, *Acc. Chem. Res. 39*, 671−679.
60. Sengupta, P., Garai, K., Sahoo, B., Shi, Y., Callaway, D. J., and Maiti, S. (2003) The amyloid beta peptide (Abeta(1−40)) is thermodynamically soluble at physiological concentrations, *Biochemistry 42*, 10506−10513.
61. Dedeoglu, A., Cormier, K., Payton, S., Tseitlin, K. A., Kremsky, J. N., Lai, L., Li, X., Moir, R. D., Tanzi, R. E., Bush, A. I., Kowall, N. W., Rogers, J. T., and Huang, X. (2004) Preliminary studies of a novel bifunctional metal chelator targeting Alzheimer's amyloidogenesis, *Exp. Gerontol. 39*, 1641−1649.
62. Ferrada, E., Arancibia, V., Loeb, B., Norambuena, E., Olea-Azar, C., and Huidobro-Toro, J. P. (2007) Stoichiometry and conditional stability constants of Cu(II) or Zn(II) clioquinol complexes; implications for Alzheimer's and Huntington's disease therapy, *Neurotoxicology 28*, 445−449.
63. Di Vaira, M., Bazzicalupi, C., Orioli, P., Messori, L., Bruni, B., and Zatta, P. (2004) Clioquinol, a drug for Alzheimer's disease specifically interfering with brain metal metabolism: structural characterization of its zinc(II) and copper(II) complexes, *Inorg. Chem. 43*, 3795−3797.
64. Blasie, C. A., and Berg, J. M. (2004) Entropy-enthalpy compensation in ionic interactions probed in a zinc finger peptide, *Biochemistry 43*, 10600−10604.
65. Krezel, A., and Maret, W. (2006) Zinc-buffering capacity of a eukaryotic cell at physiological pZn, *J. Biol. Inorg. Chem. 11*, 1049−1062.
66. Walkup, G. K., and Imperiali, B. (1997) Fluorescent chemosensors for divalent zinc based on zinc finger domains. Enhanced oxidative stability, metal binding affinity, and structural and functional characterization, *J. Am. Chem. Soc. 119*, 3443−3450.
67. Kowalik-Jankowska, T., Ruta, M., Wisniewska, K., and Lankiewicz, L. (2003) Coordination abilities of the 1−16 and 1−28 fragments of beta-amyloid peptide towards copper(II) ions: a combined potentiometric and spectroscopic study, *J. Inorg. Biochem. 95*, 270−282.

BI701355J